# Three-level nonlinear selective reflection at a glass–Cs-vapor interface

A. Amy-Klein, S. Saltiel,* O. A. Rabi, and M. Ducloy
*Laboratoire de Physique des Lasers, U.R.A. 282 du CNRS, Université Paris-Nord, 93430 Villetaneuse, France*
(Received 17 April 1995)

We present an experimental study of nonlinear selective reflection at a dielectric–Cs-vapor interface, in a three-level cascade-up scheme. The nonlinear reflection at the Cs $D_2$ resonance line is monitored in the presence of resonant irradiation at 621 nm or 658 nm ($6P_{3/2} \rightarrow 8D_{5/2}, 9S_{1/2}$). Experimental reflection spectra with either counterpropagating or copropagating light beams are analyzed and compared with the theoretical predictions of F. Schuller *et al.* [Phys. Rev. A **47**, 519 (1993)]. For a blue-detuned pump and copropagating geometry an alternative type of three-level coherent reflection resonances, specifically associated with desorbing atoms, is observed. Also observed is the nonlinear reflection associated with the off-resonant, two-photon dispersion of atoms moving parallel to the window surface. Probe beam saturation is responsible for the appearance of additional resonant features in reflection spectra. Finally we analyze crossover spectral resonances which arise from nondegenerate, four-wave-mixing processes induced by the combined influence of counterpropagating pump and probe beams, and the pump beam being partially reflected by the window.

PACS number(s): 42.65.−k, 32.80.Wr, 42.25.Gy

## I. INTRODUCTION

Selective reflection (SR) is an old spectroscopic field [1]. It has recently regained interest particularly since it has been shown that it can exhibit sub-Doppler features, when the reflection of light is monitored at normal incidence on the interface between a dielectric window and a *low-density vapor* [2]. In particular, frequency-modulated selective reflection has been demonstrated as a powerful means of monitoring long-range interactions between excited atoms and solid-state surfaces [3,4].

Nonlinear selective reflection spectroscopy in *up-cascade three-level* systems has been studied recently both theoretically [5] and experimentally [6]. The modification of the refractive index of a vapor, induced by a pump beam resonant with a transparent atomic transition between the resonance level and an upper excited state (Fig. 1), has been demonstrated on caesium vapor [6] by monitoring the reflectivity change of a probe beam that is tuned on the resonance transition. In these studies, the pump beam is either copropagating or counterpropagating with the probe beam (Fig. 2).

Several resonances are predicted [5] in three-level selective reflection at *normal incidence*:

(i) A reflectivity change at the center of the resonance transition. This resonance originates in the singular contribution to the probe beam reflectivity associated with atoms that are moving parallel to the surface (the contribution is saturated by the pump, independently of its own frequency).

(ii) A coherent three-level resonance associated with the velocity-selective cross-saturation induced by the pump beam. The center of this coherent two-photon-induced resonance is imposed by the frequency of the pump via a velocity-selection process [7]. This resonance is observed for a *blue-detuned* pump only, independently of the experimental geometry (the pump is either copropagating or counterpropagating with the probe beam). Resonances (i) and (ii) have been observed before and described in Ref. [6].

(iii) There is a third resonance predicted in nonlinear three-level reflection spectroscopy [5], which is related to *off-resonant* two-photon dispersion of the vapor. In the same way as in linear reflection, there is a singular sub-Doppler contribution to two-photon reflection associated with atoms moving parallel to the surface, and satisfying the resonance condition $\omega_s + \omega_p = \omega_1 + \omega_2$ (see Fig. 1). The observation of this two-photon reflection signal will be described in more detail in this article.

In addition, we will discuss the appearance of resonances induced by *probe beam saturation* in three-level reflection, as well as the effect of a partially standing pump wave, such as the one produced by the pump reflection on the interface (in the case of a *counterpropagating* geometry). We will show that selective reflection allows one to monitor nondegenerate, non-phase-matched, four-wave-mixing processes as crossover resonances in four-level systems.

## II. EXPERIMENTAL SETUP AND METHODOLOGY OF THE EXPERIMENT

Three-level SR experiments have been performed on both the $6S_{1/2}(F=4)$-$6P_{3/2}$-$8D_{5/2}$ and $6S_{1/2}(F=4)$-$6P_{3/2}$-$9S_{1/2}$ cascade transitions of Cs (Fig. 3): the first transition is the

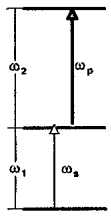


FIG. 1. Cascade three-level system. The pump beam with frequency $\omega_p$ is resonant with the upper transition (resonance frequency $\omega_2$), while the probe beam with frequency $\omega_s$ is resonant with the lower transition (resonance frequency $\omega_1$).

*Permanent address: Physics Department, University of Sofia, 1164 Sofia, Bulgaria.

 

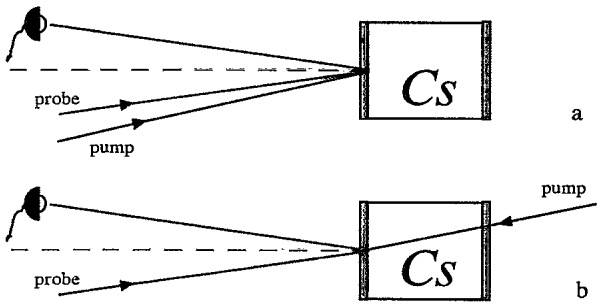


FIG. 2. Basic idea of the experiment: (a) copropagation geometry, (b) counterpropagation geometry.

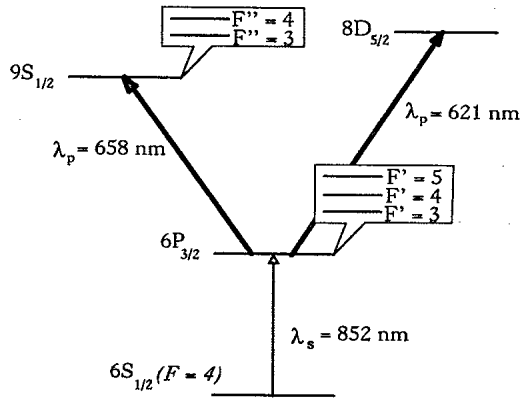


FIG. 3. Caesium $6S$-$6P$-$8D$ and $6S$-$6P$-$9S$ cascade transitions used in the experiments, with the relevant sublevel structures.

resonance line at 852 nm, the second one is in the red part of the optical spectrum at 621 or 658 nm, respectively. The total decay rates are $A_1=5.3$ MHz for $6P_{3/2}$, $A_2=1.1$ MHz for $8D_{5/2}$ (with a branching ratio of 65% to the intermediate level), and 1.0 MHz for $9S_{1/2}$ (with a branching ratio of 45% to $6P_{3/2}$) [8]. The hyperfine structure of the $8D_{5/2}$ level (about 9.3 MHz between $F''=4$ and $F''=6$ [9]) is not resolved in our experiment. The much bigger spectral distance between $9S_{1/2}$ ($F''=3,4$) sublevels (440 MHz [9]) allowed us to select spectrally the $F''=4$ hyperfine level. The infrared (IR) probe beam is provided by a frequency-stabilized laser diode with a typical 10-mW output power at 852 nm. The diode cavity is coupled via a weak optical feedback to an external confocal Fabry-Pérot cavity in order to reduce the laser jitter well below 1 MHz [10]. The pump laser source is a single-mode ring dye laser emitting in the red; its jitter is less than 1 MHz.

Both IR (probe) and red (pump) resonant beams are incident at small angles at the interface between a dielectric window (glass) and the Cs vapor (Fig. 2). We study the modification of the reflection coefficient of the IR probe beam induced by the presence of the red pump beam. In most cases, this contribution is isolated from the main part of the reflection coefficient by standard amplitude modulation techniques: the pump beam is mechanically chopped at 1.7 kHz for lock-in detection of the modulation induced in the probe reflection. In a few experiments the pump is not modulated and the probe beam is frequency modulated (FM); one then monitors the amplitude modulation (AM) induced in the probe beam reflection. In all experiments, the IR probe frequency is scanned continuously over the hyperfine transitions of the resonance line, while *the pump frequency is fixed* and quasiresonant with the upper transition. Several IR spectra can thus be recorded with the pump frequency being changed step by step.

In order to monitor the spectral positions of the SR nonlinear peaks and to compare them with the theory, we need absolute frequency references for both IR and red lasers. This is achieved with two side setups (Fig. 4). The first one consists of a conventional saturated-absorption experiment (IR-IR SA) on the Cs resonance line, which provides an absolute calibration of the IR frequency scale. With this way we determine $\Delta_s=\omega_s-\omega_1$ as the IR frequency detuning with respect to the $6S_{1/2}(F=4)$-$6P_{3/2}(F'=5)$ transition [see Fig. 5(a)]. The second setup is a three-level saturated-absorption "volume" experiment (R-IR SA): part of the IR beam and of the red beam are counterpropagating in an auxiliary Cs cell. From standard three-level spectroscopy in gas cells [7], we know that the IR transmission spectrum has a peak when IR detuning is $\Delta_s=-(k_s/k_p)\Delta_p$, where we define $\Delta_p=\omega_p-\omega_2$ as the pump frequency detuning with respect to the $6P_{3/2}(F'=5)$-$8D_{5/2}$ or $6P_{3/2}(F'=5)$-$9S_{1/2}(F''=4)$ transition ($k_s$ and $k_p$ are the probe and pump-wave vectors, respectively). The resonance center [Fig. 5(c)] allows us to monitor the exact value of $\Delta_p$.

Note that two red pump beams with exactly opposite directions of propagation are incident on the SR cell: either one or the other is blocked in order to perform either the copropagating or counterpropagating geometry experiment. The complete experimental setup is shown in Fig. 4. The three signals are detected simultaneously, and the data are memorized with the computer, which controls the diode laser frequency scanning. Both IR-IR SA and R-IR SA cells are low-pressure ones (room temperature) to achieve IR transmission of about 50%. The atomic density in the SR cell is a few $10^{13}$ atoms/cm$^3$. The diam of both beams are typically 2.5 mm and their intensity can be changed continuously with variable attenuators up to 3 mW for IR and to 40 mW for red. Typical simultaneously recorded IR-IR SA, R-IR SA, and SR experimental spectra are presented altogether in Fig. 5.

## III. EXPERIMENTAL RESULTS AND DISCUSSION

### A. Low probe intensity

SR spectra for low probe intensity and *copropagating* geometry are presented in Fig. 6. All spectra were recorded in the same experimental conditions; only the pump detuning $\Delta_p$ has been changed. Depending on this detuning, the following peaks can be observed: (i) a peak that we will designate as peak ($A$), at the detuning $\Delta_s=-(k_s/k_p)\Delta_p$, and that appears only for $\Delta_p>0$, (ii) a peak ($B$) at $\Delta_s=0$, and (iii) a peak ($C$) at $\Delta_s=-\Delta_p$ observable only when $\Delta_p<0$. This last resonance is very small and for its observation we had to use relatively higher red and IR power. Note that we observed the same peaks in the counterpropagating geometry.

Let us now investigate each resonance separately:

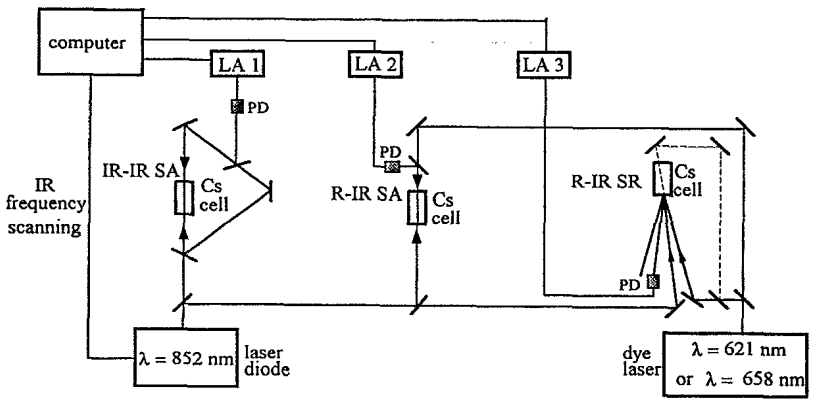


FIG. 4. Experimental setup: SR, selective reflection; SA, saturated absorption; LA, lock-in amplifier; PD, photodiode.

### 1. $\Delta_s=0$ resonance

The ($B$) peak appears at position $\Delta_s=0$ whatever the $\Delta_p$ value is, but its shape is changing from a normal dispersion ($\Delta_p>0$) to a inverted dispersion line shape ($\Delta_p<0$). At $\Delta_p\approx 0$, it looks more like an absorption line shape, with dips in both wings. The linewidth (distance between minimum and maximum) is the same for both the $6S$-$6P$-$8D$ and $6S$-$6P$-$9S$ cascade transitions, and for both cases $\Delta_p<0$ or $\Delta_p>0$. The ($B$) amplitude increases linearly with both pump and probe powers and decreases with increasing detunings $|\Delta_p|$. These experimental results are in very good agreement with the theoretical spectra derived by Schuller, Gorceix, and Ducloy [5], for this particular case of low probe intensity. This resonance, as it appears at line center ($\Delta_s=0$), is associated with atoms moving parallel to the interface (i.e., $v_z=0$, where $v_z$ is the velocity component normal to the surface). We know from linear-selective reflection analysis that a singular contribution to probe reflectivity is associated with those atoms. This singularity is saturated by the pump, and yields this ($B$) resonance, which depends on both pump and probe beams. Moreover the theory indicates that the linewidth for $\Delta_p\neq 0$ is essentially $A_1$ (with a small correction depending on $A_2$). This yields the value $A_1=15$ MHz ($\pm 2$ MHz). The difference between this value and the 5-MHz radiative linewidth can be attributed to pressure, power, and angular broadening factors [6].

### 2. Velocity-selective coherent three-level resonance

For $\Delta_p>0$ another resonance, the ($A$) peak, is observed. Its study was performed in [6], so we will just briefly review the results. The ($A$) amplitude is approximately one order of magnitude larger than ($B$) amplitude. The ($A$) resonance po-

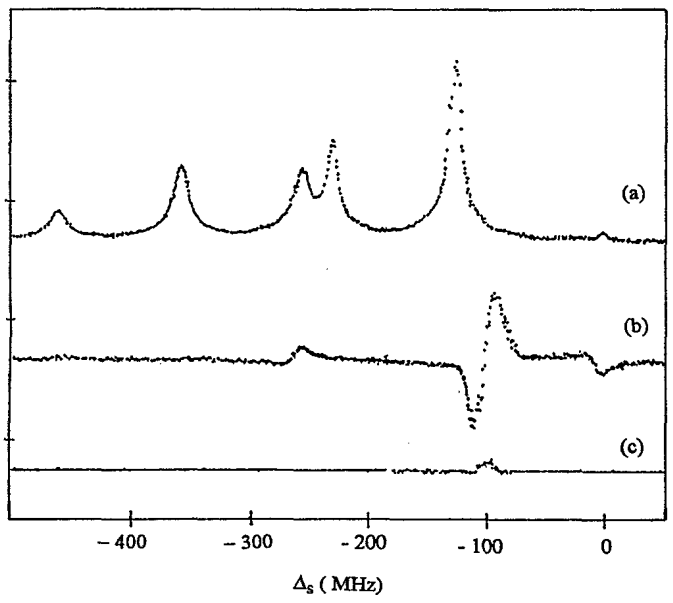


FIG. 5. Simultaneous recording of IR-IR SA (a), SR (b), and R-IR SA (c) spectra for the $6S$-$6P$-$9S$ cascade transition and copropagation geometry. Positions of the peaks in spectrum (a) are used for calibration of the $\Delta_s$ scale, while spectrum (c) is used for obtaining the pump frequency detuning $\Delta_p$. For the spectra in the figure, $\Delta_p=130$ MHz.

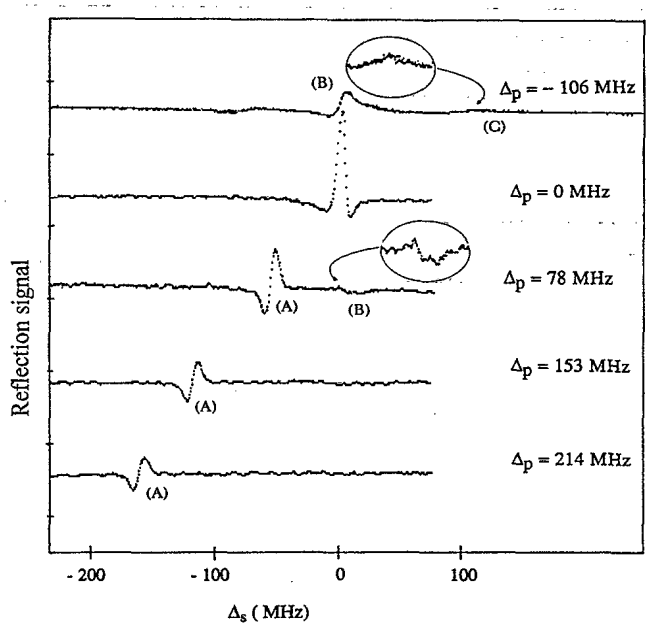


FIG. 6. Selective reflection spectra for the $6S$-$6P$-$9S$ cascade transition and copropagation geometry for different values of pump frequency detuning $\Delta_p$. The three-level resonance is indicated by ($A$), the "$\Delta_s=0$" resonance by ($B$), and the two-photon peak at position $\Delta_s=-\Delta_p$ by ($C$).

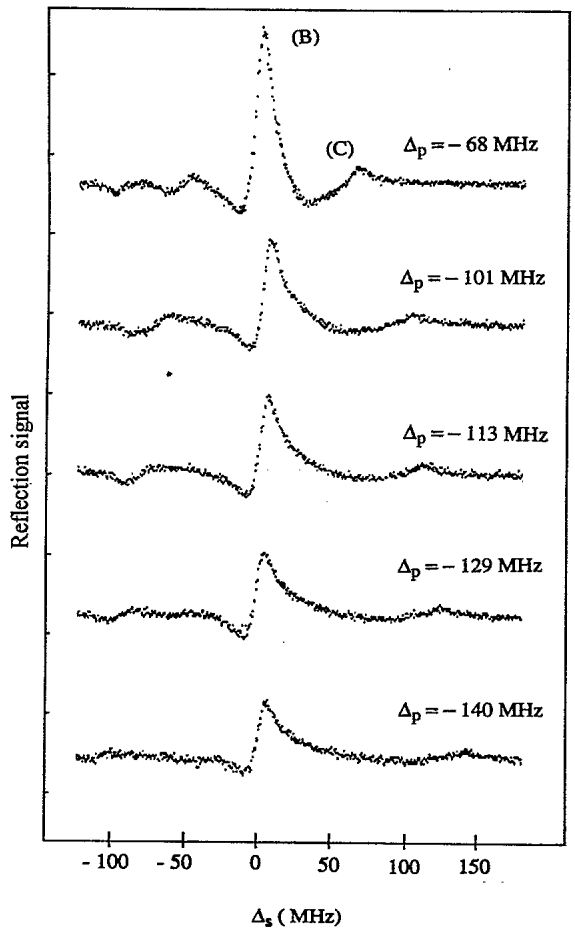


FIG. 7. Selective reflection spectra for different negative values of $\Delta_p$. The spectra are recorded with the $6S$-$6P$-$9S$ cascade transition and copropagation geometry.

sition and shape are in agreement with the Schuller, Gorceix, and Ducloy predictions [5]. This resonance originates in the atoms selected by the frequency-fixed pump beam: for the *counterpropagating* geometry, the pump beam is resonant with atoms arriving onto the surface, and for the *copropagating* geometry, with atoms leaving the surface. In the latter case, these departing atoms are in a transient interaction regime [6]. Let us recall that in all other types of spectroscopic approach (linear SR, saturated absorption in reflection [11], etc.) *the contribution of the desorbing atoms is either very small or cannot be distinguished from the contribution of the arriving atoms*. Thus this nonlinear resonance is of an alternative type in SR spectroscopy: it reflects only the contribution of atoms leaving the surface. Moreover one expects that its peak-to-peak amplitude is proportional to the atomic density in the velocity class selected by the pump beam. This allows us to monitor the velocity distribution of atoms arriving at or departing from the surface. The power of this experimental technique was demonstrated in [6] for both the $6S$-$6P$-$8D$ and $6S$-$6P$-$9S$ cascade transitions of Cs. Specifically it was shown that very close to the dielectric surface, the atomic density exhibits anomalous behavior for low normal velocities.

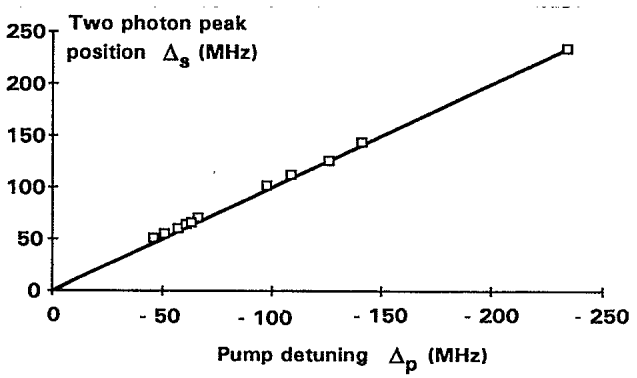


FIG. 8. Position of the two-photon selective reflection signal as a function of the pump frequency detuning $\Delta_p$. Open squares yield the experimental data, while the solid line represents the theoretical prediction. The cascade transition and beam geometry are the same as for spectra shown in Fig. 7.

### *3. Off-resonant, two-photon reflection signal*

For negative pump frequency detuning we observed another resonance [the $(C)$ peak] at position $\Delta_s = -\Delta_p$ (see Figs. 7 and 8). The amplitude of this peak is lower in comparison to the previously described ones, and we were able to detect it mainly at relatively high pump and probe beam intensities, and *with a counterpropagating* geometry for the $6S$-$6P$-$9S$ cascade transition. For copropagating geometry, and also for the $6S$-$6P$-$8D$ cascade transition, this peak was more difficult to observe at our noise level. The $(C)$ peak appears when pump and probe detunings satisfied $\Delta_p + \Delta_s = 0$ (Fig. 8), and is naturally assigned to the two-photon off-resonant $6S \rightarrow 9S$ transition. This resonance, but with higher amplitude (at least five times more), is predicted in the theoretical spectra [5] as the *two-photon coherent response of atoms moving along the surface*, i.e., atoms with a small normal velocity component. The experimentally measured width of this two-photon coherence peak is consistent with the theoretical predictions, $\sqrt{A_2 \Delta_p}$ with $A_2$ the upper-level decay rate [5]. Its amplitude decreases like $1/\Delta_p$—as usual in two-photon spectroscopy—and for $\Delta_p > 100$ MHz becomes comparable to the detection noise. The fact that the $(C)$ peak was barely seen with the $6S$-$6P$-$8D$ system can be justified by the larger value of $A_2$ for this system ($A_2 \approx A_1$) as compared to the $6S$-$6P$-$9S$ system ($A_2 \approx A_1/4$). Thus we expect the two-photon peak to be narrower for $6S$-$6P$-$9S$ (width proportional to $\sqrt{A_2}$) and then easier to distinguish from the nearest $(B)$ resonance and from noise. The discrepancy between the experimental amplitude and the theoretical predictions could be attributed to two phenomena that were not taken into account in the theory [5]: (i) probe saturation, which induces resonances (see below), masking this $(C)$ peak; (ii) surface effects; for instance, the van der Waals potential acting on upper atomic states: the slow atoms that are responsible for the two-photon resonance must be very sensitive to them.

Further development should be to analyze, theoretically and experimentally, the influence of van der Waals potential forces on this resonance. For that purpose, frequency modulation of the pump beam would be a means to get higher

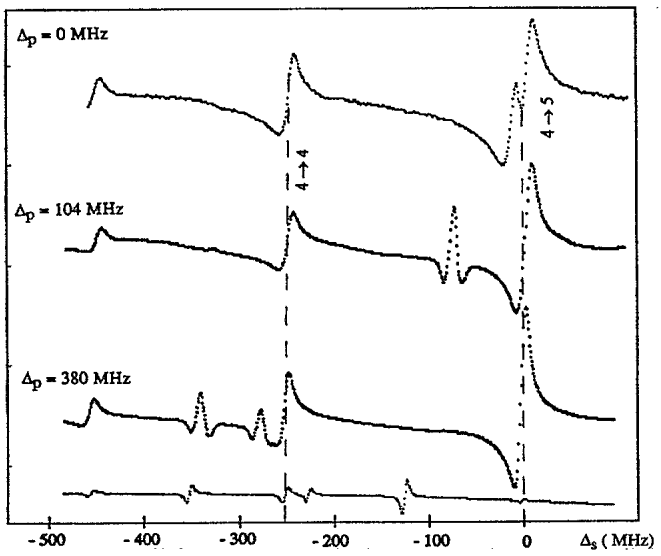


FIG. 9. Reflection spectra with FM probe. Dashed lines indicate the $F=4\rightarrow F'=4$ and $F=4\rightarrow F'=5$ sublevel resonances of the $6S$-$6P$ transition. The three-level resonant SR peak is positioned at $\Delta_s=-(k_s/k_p)\Delta_p$ and has an absorptionlike shape. The lowest recording is the reference IR-IR SA spectrum.

sensitivity. With this approach, the $(C)$ peak, which depends crucially on $\Delta_p$, should get narrower and larger, while the ($\Delta_p$-independent) $(B)$ peak is reduced. Thus the signal sensitivity to this two-photon resonance would be enhanced [12].

### B. FM probe spectra

Three-level SR spectroscopy can also be performed with *frequency modulation of the probe beam.* In this regime, the observed spectra consist of both the *linear* two-level SR signal due to interaction of the FM probe beam with the lower transition of the cascade system, and the *nonlinear* SR signal that appears only when pump and probe are present simultaneously. The overlap of the two spectra (see Fig. 9) provides internal frequency calibration of the observed spectra. The 4-3, 4-4, and 4-5 hyperfine components of the $D_2$ line are clearly seen in all of the spectra. The nonlinear SR peak is observed at position $\Delta_s=-(k_s/k_p)\Delta_p$ and has absorptionlike shape, for $\Delta_p\neq 0$. SR spectra obtained with the FM probe beam for the case $\Delta_p=0$ exhibit a splitting of the SR peak, which is similar to the dynamic Stark splitting observed in three-level transmission spectroscopy [7]. This splitting increases with increasing pump power. However, off-resonance, the $\Delta_s=0$ FM-SR resonance is light-shifted for large pump intensities.

### C. Influence of sublevel structure and crossover resonances

Our experimental study is not restricted to a pure three-level system, because of the hyperfine structure of each level. In this subsection we present and discuss results that demonstrate the influence of the hyperfine structure on the observed spectra.

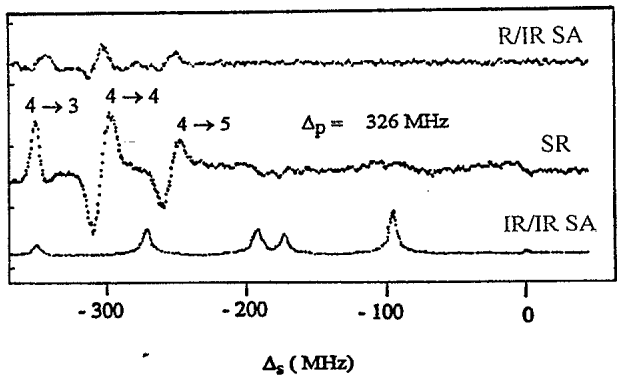


FIG. 10. Simultaneous recording of IR-IR SA, SR, and R-IR SA spectra for the $6S$-$6P$-$9S$ cascade transition, copropagation geometry, and a large positive value of $\Delta_p$. The SR spectrum consists of three resonances associated with hyperfine transitions of the caesium $D_2$ line.

#### *1. Hyperfine structure*

First we notice that in the experiments presented here, the probe beam is always tuned around $6S_{1/2}(F=4)\rightarrow 6P_{3/2}$; the other ground-state hyperfine level ($F=3$) is far away (9.19 GHz) and does not influence the observed spectra. On the contrary, the distance between $6P$ sublevels is comparable to the Doppler width ($\sim$200 MHz). Thus for certain values of $\Delta_p$ we recorded entangled spectra with several $(A)$ and $(B)$ peaks for each transition. Such a spectrum is shown in Fig. 10. For $9S_{1/2}$ it is even more complex because the $6P(F'=5)$-$9S(F''=4)$ frequency is approximately equal to the $6P(F'=3)$-$9S(F''=3)$ frequency (Fig. 3). The influence of $8D$ hyperfine structure is quite different: the sublevel intervals are small (4 and 5 MHz between $F''=4$, 5, and 6) compared to the resonance width. Thus the structure is not resolved but induces an $(A)$ peak broadening: the linewidth is approximately 6 MHz broader for $8D$ than for $9S$ [13].

#### *2. Four-wave-mixing-induced crossover resonances*

It is well known that in ordinary volume spectroscopy the sublevel structure can introduce *crossover* (CO) resonances. In general, these resonances are related to the velocity-selective cross-saturation of two coupled transitions [7]. We demonstrate here the existence of a crossover resonance of a different type in nonlinear SR spectroscopy for the $6S$-$6P$-$9S$ cascade transition, in a counterpropagating geometry. We show that these resonances originate in *volume* four-level four-wave mixing in a thin layer next to the surface.

In Fig. 11(a) SR spectra are shown for different positive detunings $\Delta_p$. In addition to the $(A)$ and $(B)$ peaks that we discussed previously, one clearly sees a peak at $\Delta_s=-97$ MHz, *whose center frequency does not depend on* $\Delta_p$ (but the amplitude does). Numerically this detuning is equal to $\Delta_s^{co}=-(k_s/k_p)\omega_{4-5}/2$, where $\omega_{4-5}$ is the $6P(F'=4)$-$(F'=5)$ sublevels frequency splitting. Note that the amplitudes are maximum when $\Delta_p=\omega_{4-5}/2$ [14].

To interpret these resonances, let us consider the *four-level* system shown in Fig. 12, formed by ground state **g**, upper state **e**, and two close sublevels **r** and **r'** (with $E_r>E_{r'}$). This four-level system is irradiated by three

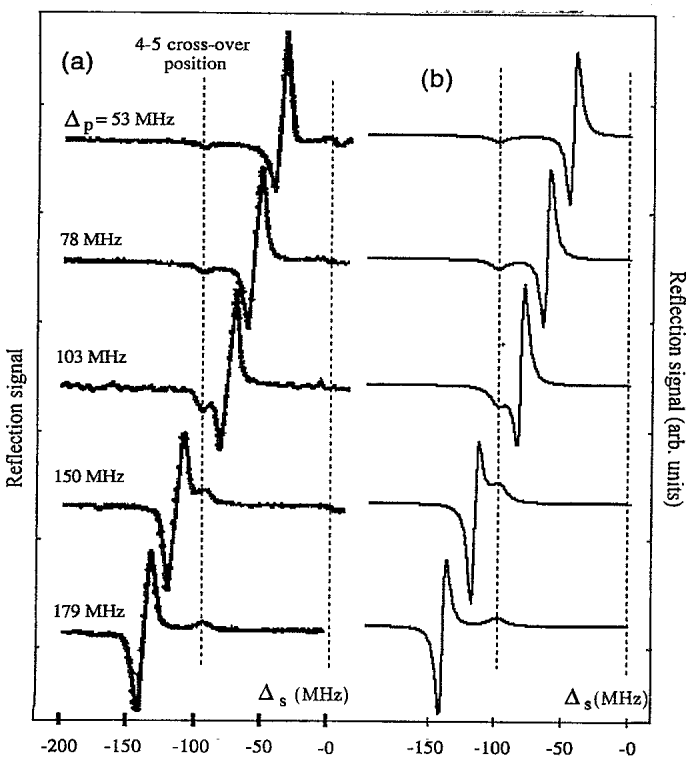


FIG. 11. (a) Experimental SR spectra for the $6S$-$6P$-$9S$ cascade transition and counterpropagating geometry. A crossover resonance peak is seen at position $\Delta_s=-97$ MHz. (b) Theoretical spectra obtained with the theory presented in the Appendix.

beams: the probe beam, the counterpropagating pump beam, and a red beam of direction $-\vec{k}_p$, that results from the 4% pump intensity reflection at the Cs-glass interface [see Fig. 2(b)] [15]. The superposition of both red beams induces a grating (parallel to the interface) on which the probe beam is diffracted: this diffracted beam is superimposed onto the probe specular reflection, as is the SR beam. This nondegenerate four-wave-mixing resonance arises from the following process: one probe photon absorption ($g\rightarrow r$ transition), one pump photon absorption ($r\rightarrow e$ transition), and stimulated emission of one reflected pump photon ($e\rightarrow r'$ transition). This leads to the emission of one photon in the direction of the reflected beam ($r'\rightarrow g$ transition). The velocity-selection rules can then be written as (we take $k_p=|\vec{k}_p|$):

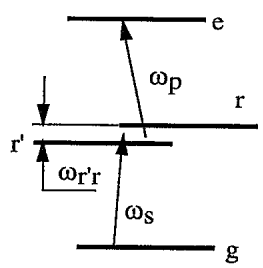


FIG. 12. Four-level system formed by ground state **g**, excited state **e**, and two close sublevels **r'** and **r** split by frequency $\omega_{r'r}$.

$$\Delta_p=\omega_p-\omega_{re}=\vec{k}_p\cdot\vec{v}=-k_pv_z,$$

$$\Delta_{p'}=\omega_p-\omega_{r'e}=-\vec{k}_p\cdot\vec{v}=k_pv_z,$$

$$\Delta_s=\omega_s-\omega_{gr}=\vec{k}_s\cdot\vec{v}=k_sv_z.$$

This yields the resonance position $\Delta_s^{co}=(k_s/k_p)\times(\Delta_{p'}-\Delta_p)/2=-(k_s/k_p)\omega_{r'r}/2$ and the velocity class contributing to the signal $v_z=\Delta_s/k_s=-\omega_{r'r}/2k_p$. Note that this velocity is *negative*: the resonance arises from atoms arriving at the surface, i.e., that are in a stationary state of interaction with the e.m. fields, as for a *volume* resonance [16].

We emphasize that this four-wave-mixing process is not phase matched: the diffracted beam has the wave vector $\vec{k}^{co}=-\vec{k}_s+\Delta\vec{k}$ with $\Delta\vec{k}=2(\vec{k}_p+\vec{k}_s)$, i.e., $\Delta k=2|k_s-k_p|$. Thus the volume signal originates only in the layer next to the interface, whose width is $\Delta z^{co}=\pi/\Delta k\approx 720$ nm. This *volume* CO resonance originates in an atomic vapor layer comparable to the SR *surface* layer (let us recall that SR resonance takes place in the thin layer of depth $\pi/2k_s\approx 210$ nm). This basically explains why both phenomena have the same order of magnitude. We present in the appendix a detailed derivation of the CO resonance line shape and compare CO and SR amplitudes. The resulting theoretical spectra fit the experimental ones well, as can be seen in Fig. 11(b).

Finally, we remark that the observation of four-wave-mixing resonances implies both an isolated four-level system and a counterpropagating geometry, and thus was only performed with a $6S$-$6P$-$9S$ counterpropagating experiment.

### D. Saturation-induced extra resonances

When we increase the pump power we observe line broadening without any measurable asymmetries. No pump-induced amplitude saturation occurs up to values of 35 mW. However, in the copropagating geometry, the increase of probe power has a very strong influence: in addition to broadening and saturation effects, different resonances have been observed.

(i) We observe a different behavior for the amplitude dependence of resonances ($A$) and ($B$) as functions of the probe power. The ($A$) peak-to-peak amplitude depends linearly on probe power until a few mW, while the ($B$) peak-to-peak amplitude saturates at around 0.7 mW.

The two different saturation intensities have to be attributed to the different origin of the two resonances, as already noted in [17]. Indeed, the resonance ($A$) originates exclusively in atoms leaving the surface, which thus do not spend enough time in the beam to experience saturation.

(ii) When probe power exceeds 50 $\mu$W, an additional resonance appears in the reflection spectra for negative $\Delta_p$. One observes a dispersive resonance at $\Delta_s=(k_s/k_p)\Delta_p$ for copropagating geometry that we labeled the ($R$) peak (Fig. 13). Its amplitude, $I_R$, depends linearly on pump power $I_p$. However, it depends first quadratically and then linearly on probe power $I_s$ (Fig. 14). This dependence can be fitted by the following formula:

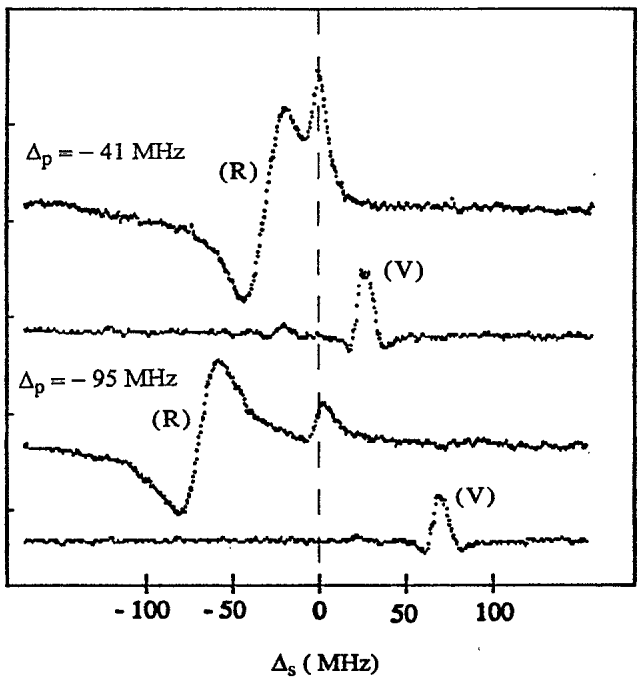


FIG. 13. SR spectra obtained with saturating probe and copropagating geometry. A resonance ($R$) is observed at position $\Delta_s=(k_s/k_p)\Delta_p$. The three-level volume resonance ($V$) is obtained with the R-IR SA side setup (see Fig. 4) and is centered at $\Delta_s=(k_s/k_p)\Delta_p$.

$$I_R \propto \frac{I_p I_s^2}{1+I_s/I_0},$$

where $I_0$ is the probe saturation intensity.

We note that this resonance corresponds to a selection, by the pump beam, of atoms arriving onto the surface and which are in steady-state interaction with light beams. This situation is similar to conventional three-level volume saturated absorption. Indeed, it is known in three-level saturation spectroscopy [7] that for that geometry there is no pump-induced signal at low probe power in the Doppler limit approximation. However, when the probe power is high enough to saturate the susceptibility or to populate the intermediate level, one observes a nonlinear response that depends quadratically on probe intensity [18]. Resonance ($R$) originates from the contribution of this saturation mechanism to the refractive index [19].

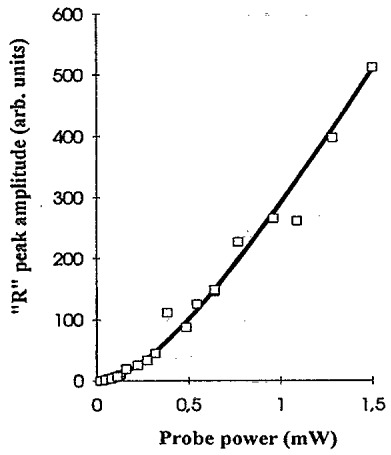


FIG. 14. Peak-to-peak amplitude of the "$R$" peak as a function of the probe power. Open squares are the experimental data. Solid line is the fit (see text).

This interpretation was corroborated by numerical calculations of F. Schuller [20], who extended the theoretical approach of Ref. [5] to arbitrary probe power. The experimental spectra (Fig. 13) and probe power dependence reproduce the prediction of this approach quite well.

Resonance ($R$) is the signature for saturation-induced breaking of the equivalence between copropagating and counterpropagating geometries. This symmetry breaking arises for large probe power ($\Omega_s > A_1, A_2$).

## IV. CONCLUSION

The experimental study of selective reflection on Cs vapor in a pump-probe scheme has allowed us to observe the main characteristics of three-level reflection spectroscopy, and analyze the properties of the atomic response as a function of the beam geometry: transient three-level response of desorbing atoms for copropagating beams *versus* steady-state atomic response for counterpropagating beams. Two-photon selective reflection has been monitored. We have observed and interpreted a crossover resonance connected to the partial standing-wave character of the pump field (for a counterpropagating geometry), as well as saturation-induced extra-resonances originating in probe-induced higher-order processes. Work is now in progress to observe two-photon selective reflection in the frequency-modulated pump mode [21]. This should lead to the spectroscopic observation of atom-dielectric long-range interactions for high-lying ($nS$ or $nD$) atomic levels, and possibly to the monitoring of the frequency dispersion and birefringence of the dielectric response [22].

## ACKNOWLEDGMENTS

We acknowledge stimulating discussions with F. Schuller, D. Bloch, and O. Gorceix. We wish to thank I. Stefanov for his participation in some of the experiments. One of us (S.S.) would like to thank University Paris-Nord and Laboratoire de Physique des Lasers for their kind hospitality and support during his stay.

## APPENDIX

In this appendix we derive the crossover (CO) resonance line shape and compare the CO and SR amplitudes versus the value of $\Delta_p$.

### A. CO resonance amplitude

We consider a vapor of four-level systems (Fig. 12), irradiated by three beams:

(i) the signal beam transmitted inside the vapor

$$E_{s'} = A_{s'} \exp[i(\omega_s t - k_s z)] + \text{c.c.},$$

where $A_{s'}=[2n/(n+1)]A_s$, ($A_s$ is the amplitude of the incident probe beam in the dielectric);

(ii) the counterpropagating pump beam

$$E_p=A_p\exp[i(\omega_p t+k_p z)]+\text{c.c.};$$

(iii) the reflected pump beam

$$E_{p'}=A_{p'}\exp[i(\omega_p t-k_p z)]+\text{c.c.},$$

where $A_{p'}=[(n-1)/(n+1)]A_p$.

The Rabi frequencies $\Omega_{s'}$, $\Omega_p$, and $\Omega_{p'}$ associated with these three beams are defined as $\Omega_j=(2\mu/\hbar)A_j$. The CO beam is radiated by the induced macroscopic polarization $P(z)$

$$P(z)=N\mu(\langle\rho_{r'g}\rangle+\langle\rho_{gr'}\rangle),$$

where $N$ is the atomic density, $\mu$ is the lower transition dipole moment, and $\langle\rho_{r'g}\rangle=\int_{-\infty}^{+\infty}\rho_{r'g}(z,v_z)W(v_z)dv_z$ [$W(v_z)=(v_0\sqrt{\pi})^{-1}\exp(-v_z^2/v_0^2)$ with $v_0$ the mean thermal velocity].

For $v_z<0$, we can derive the steady-state third-order perturbative solution of the density-matrix Bloch equations under the form

$$\rho_{r'g}^{(3)}=-\frac{1}{8}\frac{i\Omega_{s'}\Omega_p\Omega_{p'}e^{i[\omega_s t-(k_s-2k_p)z]}}{(\frac{1}{2}A_1-i\tilde{\Delta}_{rg})(\frac{1}{2}A_2-i\tilde{\Delta}_{eg})(\frac{1}{2}A_1-i\tilde{\Delta}_{ger'})}, \quad \text{(A1)}$$

where

$$\tilde{\Delta}_{rg}=\Delta_s-k_s v_z,$$

$$\tilde{\Delta}_{eg}=\Delta_s+\Delta_p-(k_s-k_p)v_z,$$

$$\tilde{\Delta}_{ger'}=\Delta_s+\Delta_p-\Delta_{p'}-(k_s-2k_p)v_z.$$

For $v_z>0$, the atoms are in a transient regime of interaction with the beams. However we know from the velocity-selection rules (Sec. III C 2) that the CO resonance is observed for $\Delta_p>0$ and originates from $v_z<0$ atoms. Thus, the contribution of the departing atoms should be negligible. To perform the velocity average we thus consider (A1) as valid for any velocities. By means of the residue theorem we obtain

$$P=P_0 e^{i[\omega_s t-(k_s-2k_p)z]}+\text{c.c.}, \quad \text{(A2)}$$

where $P_0=-i(\sqrt{\pi}/8)(N\mu\Omega_{s'}\Omega_p\Omega_{p'}/v_0)(\rho/k_p)D_{co}$, and $D_{co}=1/(\gamma_a-i\Delta)(\frac{1}{2}A_1-i\Delta')$; with $\Delta=\Delta_s+\rho\Delta_p$; $\Delta'=\Delta_s+\frac{1}{2}\rho\omega_{r'r}$; $\gamma_a=\frac{1}{2}[\rho A_2+(1-\rho)A_1]$; and $\rho=k_s/k_p$.

This polarization is responsible for the emission of the CO electromagnetic wave

$$E_{co}=A_{co}e^{i(\omega_s t+k_s z)}+\text{c.c.},$$

which propagates along the reflected probe beam. We obtain the amplitude $A_{co}$ from the integral $A_{co}=i(k_s/2\varepsilon_0)\int_0^\infty P_0 e^{i(2k_p-2k_s)z}dz$, and as a result,

$$A_{co}=-i\frac{\sqrt{\pi}\rho^2}{16\varepsilon_0(\Delta k)}\frac{N\mu\Omega_{s'}\Omega_p\Omega_{p'}}{v_0}D_{co}, \quad \text{(A3)}$$

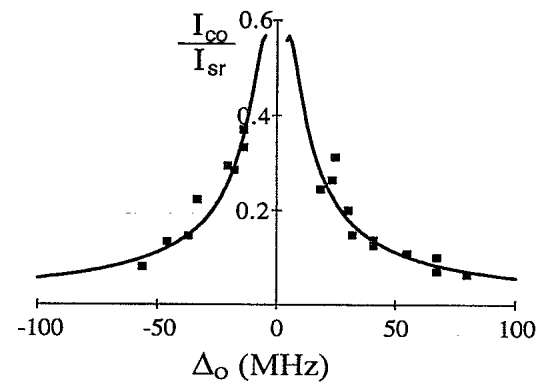


FIG. 15. Ratio of the amplitudes of the crossover (CO) resonance and the selective reflection (SR) resonance versus detuning parameter $\Delta_0$ (frequency separation between the two resonances). Experimental data, full squares; theoretical predictions, solid line.

with $\Delta k=2(k_p-k_s)$.

### B. Comparison of the CO and SR amplitudes

We monitor the heterodyne beat of both transmitted CO and SR signals, with the specularly reflected probe:

$$I=\varepsilon_0 c\left\langle\left|\frac{n-1}{n+1}E_s+\frac{2}{n+1}E_{co}+\frac{2}{n+1}E_{SR}\right|^2-\left|\frac{n-1}{n+1}E_s\right|^2\right\rangle, \quad \text{(A4)}$$

where $\langle\ \rangle$ designates the time average. We thus detect $I=I_{CO}+I_{SR}$, where

$$I_{CO}=2\varepsilon_0 c[4(n-1)/(n+1)^2]A_s\mathrm{Re}A_{CO},$$

$$I_{SR}=2\varepsilon_0 c[4(n-1)/(n+1)^2]A_s\mathrm{Re}A_{SR}.$$

$\mathrm{Re}A_{CO}$ is given by (A3), and $\mathrm{Re}A_{SR}$ may be obtained from [5] (expressed in SI units):

$$\mathrm{Re}A_{SR}=\frac{n}{n+1}A_s\mathrm{Re}T \quad \text{(A5)}$$

with

$$\mathrm{Re}T=-\frac{\sqrt{\pi}}{8}\frac{N\hbar\Omega_s^2\Omega_p^2}{\varepsilon_0 A_s^2 v_0}\frac{(1-\rho)}{k_p}\frac{\gamma_a\Delta}{(\gamma_a^2+\Delta^2)^2}.$$

Finally we get

$$I_{CO}=\frac{1}{4}\left(\frac{n-1}{n+1}\right)\frac{\rho^2}{(1-\rho)^2}K\frac{\gamma_a\Delta'+\frac{1}{2}A_1\Delta}{(\gamma_a^2+\Delta^2)(\frac{1}{4}A_1^2+\Delta'^2)} \quad \text{(A6)}$$

and

$$I_{SR}=K\frac{\gamma_a\Delta}{(\gamma_a^2+\Delta^2)^2}, \quad \text{(A7)}$$

with

$$K=-\sqrt{\pi}\frac{n(n-1)}{(n+1)^3}\frac{N\hbar\Omega_s^2\Omega_p^2}{v_0}\frac{(1-\rho)}{k_p}c.$$

The maximum SR amplitude in Doppler limit approximation does not depend on $\Delta_p$ and is given by $I_{SR}=K(3\sqrt{3}/16)1/\gamma_a^2$. The CO peak has maximum amplitude for $\Delta_p=\omega_{r'r}/2$. Otherwise its amplitude is decreasing with increasing distances $|\Delta_0|$ between the SR and CO peaks $[\Delta_0=\rho(\omega_{r'r}/2)-\rho\Delta_p]$.

The theoretical spectra shown in Fig. 11(b) are obtained with the formulas (A6) and (A7). In Fig. 15 experimental data and theoretical predictions are compared for the ratio of the CO and SR amplitudes versus detuning $\Delta_0$. To obtain the theoretical curve, we use the value $A_1=15$ MHz [6]. The best fit was obtained for the ratio $A_1/A_2=2$. Note that for very small values of $\Delta_0$, when $\Delta_p\approx\omega_{r'r}/2$ and for the parameters of this cascade system, the CO signal amplitude is practically equal to the SR signal amplitude.


[1] R. W. Wood, Philos. Mag. **18**, 187 (1909).

[2] J. L. Cojan, Ann. Phys. (France) **9**, 385 (1954); J. P. Woerdman and M. Schuurmans, Opt. Commun. **14**, 248 (1975); A. M. Akul'shin, V. L. Velichanskii, A. S. Zibrov, V. V. Nikitin, V. A. Sautenkov, E. K. Yurkin, and N. V. Senkov, Pis'ma Zh. Éksp. Teor. Fiz. **36**, 247 (1982) [JETP Lett. **36**, 303 (1982)]; M. Oria, D. Bloch, and M. Ducloy, in *Laser Spectroscopy IX*, edited by M. S. Feld *et al.* (Academic, New York, 1989), pp. 51–53.

[3] M. Oria, M. Chevrollier, D. Bloch, M. Fichet, and M. Ducloy, Europhys. Lett. **14**, 527 (1991); M. Chevrollier, D. Bloch, G. Rahmat, and M. Ducloy, Opt. Lett. **16**, 1879 (1991); M. Chevrollier, M. Fichet, M. Oria, G. Rahmat, D. Bloch, and M. Ducloy, J. Phys. II (France) **2**, 631 (1992).

[4] M. Ducloy and M. Fichet, J. Phys. II (France) **1**, 1429 (1991).

[5] F. Schuller, O. Gorceix, and M. Ducloy, Phys. Rev. A **47**, 519 (1993).

[6] O. A. Rabi, A. Amy-Klein, S. Saltiel, and M. Ducloy, Europhys. Lett. **25**, 579 (1994).

[7] I. M. Beterov and V. P. Chebotaev, in *Progress in Quantum Electronics*, edited by J. H. Sanders and S. Steholm (Pergamon, Oxford, 1977), Vol. 3, and references therein; M. Ducloy, J. R. R. Leite, and M. S. Feld, Phys. Rev. A **17**, 623 (1977).

[8] C. E. Theodosiou, Phys. Rev. A **30**, 2881 (1984).

[9] E. Arimondo, M. Inguscio, and P. Violino, Rev. Mod. Phys. **49**, 31 (1977).

[10] B. Dahmani, L. Hollberg, and R. Drullinger, Opt. Lett. **12**, 876 (1987).

[11] F. Schuller, G. Nienhuis, and M. Ducloy, Phys. Rev. A **43**, 443 (1991).

[12] We carried out calculations from the theory [5] (precisely from the appendix formula in [5]) and derived theoretical FM spectra that corroborate these arguments.

[13] In fact, the peak results from the superposition of the three resonances corresponding to $F''=4$, 5, 6 sublevels, detuned by the hyperfine distances and balanced by the coefficients 1, 7, 31 (these coefficients are proportional to the oscillatory strengths for each hyperfine transition).

[14] A resonance corresponding to the $(F'=3)$-$(F'=5)$ crossover was also observed at position $\Delta_s^{CO}=-(k_s/k_p)\omega_{3-5}/2$.

[15] This reflection also affects the SR resonance amplitude, but independently of $\Delta_p$, so we did not consider it.

[16] We remark that this volume process also induces a resonance at $\Delta_s=0$ originating from atoms with $v_z=0$. This limits the precision of the SR amplitude measurement that we detailed in [6].

[17] V. Vuletic, V. A. Sautenkov, C. Zimmermann, and T. W. Hansch, Opt. Commun. **108**, 77 (1993).

[18] A. Amy-Klein, O. Gorceix, S. Le Boiteux, J. R. R. Leite, and M. Ducloy, Opt. Commun. **90**, 265 (1992).

[19] In the copropagating geometry an additional resonance has also been observed at large probe power ($I>0.1$ mW) and when $\Delta_p$ is negative. Its position is the same as for three-level volume resonance and is given by $\Delta_s=-(k_s/k_p)\Delta_p$. Its amplitude is very weak as it originates in atoms leaving the surface, which thus are in a transient interaction regime with the light beams.

[20] F. Schuller (private communication).

[21] J. C. Keller *et al.* (private communication).

[22] M. Fichet, F. Schuller, D. Bloch, and M. Ducloy, Phys. Rev. A **51**, 1553 (1995).